Uncovering turbulence of dust particles in the Hartmann tube through the Image-Subtraction Method

Powder Technology 457 (2025) 120871

Contents lists available at ScienceDirect

Powder Technology

journal homepage: www.journals.elsevier.com/powder-technology

Uncovering turbulence of dust particles in the Hartmann tube through the Image-Subtraction Method

Luca Marmo [a,*], Olivier Dufaud [b], Fausto Franchini [c], Enrico Danzi [a]

[a] Dipartimento di Scienza Applicata e Tecnologia-Politecnico di Torino, C.so Duca degli Abruzzi 21, 10129 Torino, Italy
[b] Université de Lorraine, CNRS, LRGP, F-54000 Nancy, France
[c] Department of Energy (DENERG), Politecnico di Torino, Viale T. Michel 5, 15121 Alessandria, Italy

HIGHLIGHTS

- The Image Subtraction Method is used to study the dust cloud dynamics during flammability measurement.
- The effects of blast pressure, concentration, density, and particle size were determined.
- Ignition delay times should be varied over wide turbulence ranges during MIE testing.
- Optimum test conditions are obtained for a homogeneous cloud at reduced turbulence.
- A good indicator for defining optimal conditions of tests may be the Stokes number.

GRAPHICAL ABSTRACT

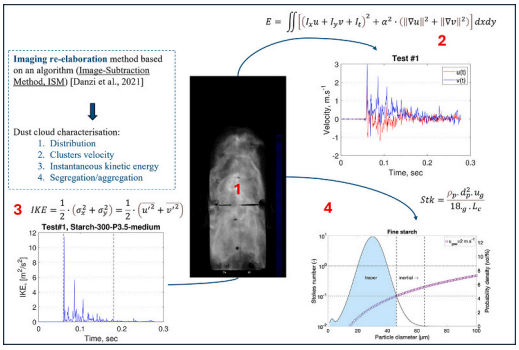

ARTICLE INFO

Keywords:
Dust explosion
Minimum ignition energy
Image processing
Instantaneous kinetic energy

ABSTRACT

The present work investigates the dynamics of dust clouds in space and time when dispersed inside the modified Hartmann tube commonly used for explosibility screening and Minimum Ignition Energy (MIE) measurement. This study focuses on the fluid dynamics of the dust cloud in the space between the electrodes where the ignition occurs since fundamental properties of the dust motion, such as the cloud turbulence (intensity and variation), are known to affect both the ignition sensitivity and explosion severity significantly. An imaging re-elaboration method based on an algorithm (Image-Subtraction Method, ISM) is presented and adopted in the basics of the present research. To clarify the cloud dynamics, a novel approach is proposed here, using LabVIEW® specific algorithms, namely Particle Analysis and optical flow detection methods, which allow the tracking of the motion and the velocity vectors of dust clusters identified in the cloud flow. Concurrently, measuring the intensity of concentration changes between the electrodes (luminance change of the video frames in time and space) and cloud velocity, which likely represents the turbulence, is possible. Different types of dust (iron, starch, silica) were used at different dispersion conditions (dispersion pressure and dust amount). The cloud motion was recorded, and videos were analyzed through LabVIEW® to explore the parameters affecting dust turbulence (powder-specific gravity, particle size distribution, and air blast intensity). The outcomes of this work will help

* Corresponding author.
E-mail address: luca.marmo@polito.it (L. Marmo).

https://doi.org/10.1016/j.powtec.2025.120871
Received 9 November 2024; Received in revised form 17 February 2025; Accepted 28 February 2025
Available online 1 March 2025

characterize the flow of a dust cloud inside a tube before its ignition and better define the optimal testing conditions for MIE determination.

1. Introduction

Because of its stochastic nature, powder dispersion is a critical step in determining ignition sensitivity or explosion severity. While international standards aim to limit data scattering by controlling operating conditions, their application cannot lead to the same state of powder dispersion (local concentration, turbulence, etc.) when the powder characteristics differ. Particularly regarding the procedure for determining the minimum ignition energy (MIE), the dust cloud dynamics have been relatively seldom investigated in the dust explosion literature [1]. This work follows previous papers [2,3], whose common goal was to identify a suitable method for studying the fluid dynamics of a dust cloud within standard ignition test equipment such as the modified Hartmann tube [4] and describe the dust concentration distribution and turbulent cloud structure. This characterization is crucial for ignition test reliability [5,6], as "optimal conditions" must be reproduced inside standard equipment to detect the MIE accurately. In the framework of an explosion risk assessment, the adjective "optimal" can refer to the actual conditions of a potential explosion event in work ambiances (i.e., the "most likely case") or conditions leading to the lowest MIE (i.e., namely, the "worst conditions possible").

Several factors influence the ignition likelihood of a combustible dust cloud, especially:

1. The dust cloud concentration and its homogeneity,
2. The cloud turbulence at ignition,
3. The ignition energy.

The theoretical optimal conditions for an explosion ignition are met for an almost stoichiometric dust cloud concentration and the lowest turbulence intensity at the ignition location. Depending on powder size, volatility, and initial oxygen content, the air/fuel ratio is sometimes a long way from theoretical stoichiometry, but optimum conditions are always achievable for a fuel equivalence ratio greater than unity. Then, MIE measurement should be carried out when the cloud is in such situations. Due to the transient behavior of the dust cloud in the modified Hartmann tube, it is essential to study aerodynamics at the ignition location to ensure optimal conditions are realized at ignition. Eventually, ignition delay time (also called t_v) may be adjusted to meet such requirements. In this light, it is necessary to provide detailed information on the dust cloud turbulence and concentration distribution in the test chamber. Since conventional MIE setups do not allow in-situ measurements, and their viewing area is limited, a reliable method to measure the latter two parameters is essential.

The investigation performed in this work is focused on the "early dispersion" stage, i.e., it is centered on the dust cloud dynamics before ignition. The standard procedures for MIE measurement [7] imply the ignition source is triggered after a specific delay from the air blast valve opening, which may be customized (usually 60, 120, or 180 ms after onset of dispersion). For this reason, this work investigates the dust cloud concentration distribution and the turbulence intensity, i.e., the intrinsic dust cloud dynamics in the modified Hartman tube, without considering the ignition interference.

Previous work by Danzi et al. [2,3], Pan et al. [8], and Puttinger et al. [9], has demonstrated the transient behavior of the cloud structure during the earliest dispersion stage. The cloud structure is influenced by dust concentration, characteristics (i.e., nature, shape, particle size distribution - PSD), and blast pressure, affecting the cloud's turbulence. As a consequence, these variables affect the ignition effectiveness. This paper focuses on the impact of some of these variables on dust cloud turbulence, which is described by the turbulence intensity and kinetic energy at the ignition location and during cloud dispersion.

2. Experiments

High-speed videos (2000 fps acquisition rate) of a dust cloud dispersion in a cylindrical modified Hartmann tube were acquired under various experimental conditions. Different powders were used to study the effect of the PSD and density on the cloud behavior: iron powder, maize starch, and silica, although the latter powder is not flammable. Silica and iron powders were available in two different PSDs (coarse and fine). Powder characteristics are listed in Table 1.

2.1. Optical setup configuration

This work adopted the same video acquisition method and data post-treatment technique used by Danzi et al. [2,3]. A simplified diagram of the experimental setup is provided in Fig. 1. Dust dispersion tests were conducted in a modified Hartmann tube (MIKE3). The vessel consists of a 1.2 L cylindrical glass tube (68 mm internal diameter and 300 mm height) closed at its lower part by a dispersion cup equipped with a mushroom-shaped nozzle. The powder is placed in the cup and is then dispersed by an air blast at different pressures. Two electrodes were placed at 100 mm from the bottom of the tube to accurately reproduce the standard [4] MIE measurement test environment.

This paper presents further elaborations on the high-speed videos presented by Danzi et al. [3]. The dispersion tests are #1 to #14, as summarized in Table 1. It should be noted that the actual concentration of powder at ignition cannot be determined in advance, as it depends on the expansion of the dust cloud, which in turn depends on the dispersion dynamics and the ignition delay time. However, in the context of this study and for the conditions considered, the mass concentrations ranged from 300 to 1100 $g.m^{-3}$.

Operating conditions were varied to investigate their effect on the dust cloud dynamics. The basic test conditions were those suggested by standards for MIE measurement, however some changes to air pulse pressure were done to detect possible improvements:

- Air pulse pressure (3.5 or 7 bar_g),
- Mass dispersed (300 or 600 mg),
- Dust PSD (fine and coarse, depending on the sample - Table 1),
- Dust nature (here, mostly related to density changes).

A high-speed video camera (MotionBlitz EoSens mini2) recorded dust cloud dispersion at 2000 fps. A black screen was placed behind the Hartmann tube to limit light reflections, while a halogen lamp provided a light source to limit light intensity oscillations.

2.2. Video elaboration – image subtraction method (ISM)

ISM is adopted to elaborate the video frames [2,3]; the information collected from the post-treatment data allowed us to estimate the dust cloud motion and dust concentration gradients in time and space.

The method consists of three steps: video filtering, detection of light brightness induced by the dust in each row of the video frames, and finalization of brightness data outcomes.

The video filtering algorithm used here is called *"initial difference"*. It is a background brightness subtraction that produces clear, non-differential images of the cloud. The drawback consists of the generation of dark spots and artefacts in the areas where the background is brightest. A single bright object in the background or a reflection of the lights on the tube glass is eliminated. This calculation mode requires a

specific experimental setup (with careful light and background control). It allows the cancellation of the background without losing information on the dust clusters' movement and distribution [3].

The algorithm subtracts the brightness of the background and produces clear, defined images of the cloud. It eliminates a single bright object in the background or a reflection of lights on the glass tube. The algorithm does not alter the light signal produced by the particles. It contains no parameters subject to tuning, so it does not pose measurement sensitivity problems.

Fig. 2 presents an example of the original and elaborated videos.

2.3. Video elaboration – particles' optical flow

Optical flow is defined as the distribution of apparent velocities of a bright pattern moving in an image. It relies on the relative motion of objects and an observer. In our case, the apparent velocities are those related to a particle cluster in the dispersion tube. The particle's velocity field was calculated using the Horn and Schunck method [10]. It is an iterative implementation of an algorithm that assumes smoothness in the dust flow (represented by its global energy E) over the whole image, i.e., it minimizes distortions in flow and favors solutions that show an increased smoothness.

$$E = \iint \left[\left(I_x u + I_y v + I_t \right)^2 + \alpha^2 \bullet \left(\|\nabla u\|^2 + \|\nabla v\|^2 \right) \right] dxdy \tag{1}$$

where I_x, I_y and I_t are the image intensity derivatives, u and v are x- and y-axis velocities and α is a constant. An alternative to the Horn and Schunck method is the Lucas-Kanade method, which was not adopted since it requires small motions per frame for best results, even less than one pixel per frame. In fact, tentative attempts using the Lucas-Kanade method resulted in a very noisy speed field detection, almost unusable with the available video data.

The algorithm (Eq. 1) is implemented in LabVIEW®, whose development environment natively includes complete optical flow function libraries within the IMAQ package (Image Acquisition). The analyzed image area is located in the space surrounding the electrodes, its center corresponding to the midpoint between the electrode's tips. The analyzed area was 90 by 90 pixels wide, and the horizontal and vertical velocity components were calculated at each pixel in that area. The final traces representing the velocity evolution over time consist of the single center pixel only, which is located between the electrodes. The Horn and Schunck method is of the iterative type, and several convergence and stopping parameters can be set in the adopted function. The *"smoothness"* parameter was particularly useful in compensating for excessive noisiness in the calculation results, and it was set to a value of 10 pixels, empirically stated as the lowest value, giving optimal convergence results, meaning that a further increase of the parameter's value did not bring advantages in the convergence.

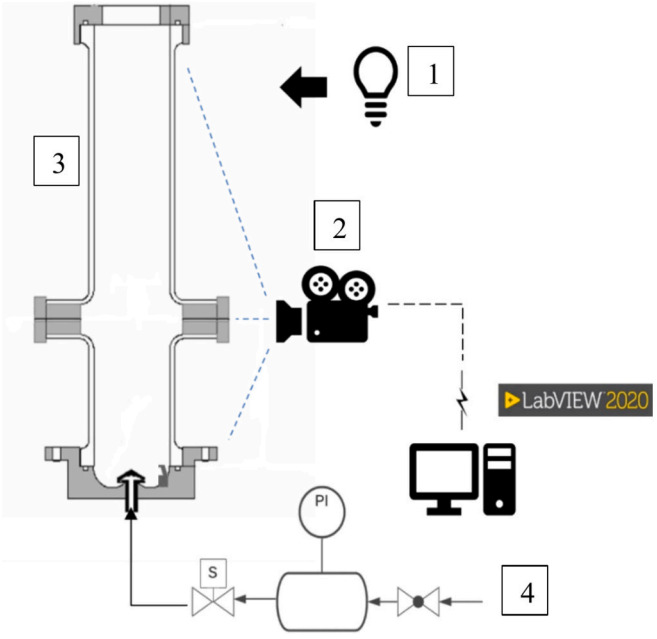

Fig. 1. Scheme of the experimental setup, where 1 stands for the illumination setup, 2 is the high-speed camera, 3 is a modified Hartman tube, and 4 is the air pulse system.

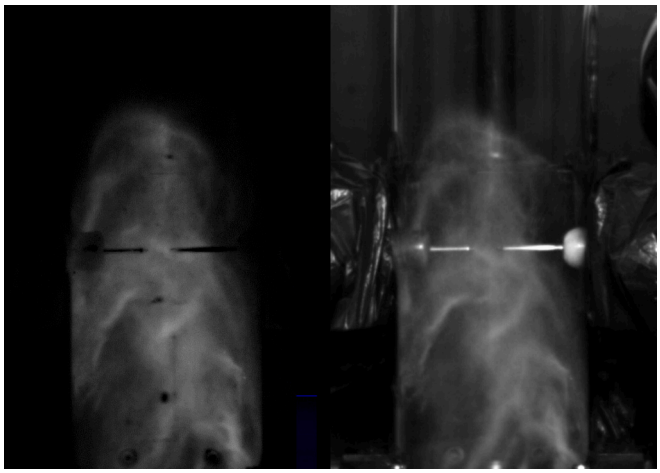

Fig. 2. Test# 10 performed on silica: InitialDifference, 80 msec (left), original video (right).

Table 1
Parameters of the dispersion tests.

Test	Dust	Mass dispersed [mg]	P [bar]	PSD [μm]			Particle size classes	Density (particle) [g/cm^3]
				d_{10}	d_{50}	d_{90}		
1	Maize starch	300	3.5	12.9	28.1	58.2	Medium	0.54
2	Maize starch	300	7	12.9	28.1	58.2	Medium	0.54
3	Maize starch	600	3.5	12.9	28.1	58.2	Medium	0.54
4	Maize starch	600	7	12.9	28.1	58.2	Medium	0.54
5	Iron	600	3.5	22.1	39.2	65.3	Coarse	7.8
6	Iron	600	7	22.1	39.2	65.3	Coarse	7.8
7	Iron	600	3.5	0.8	1.9	4.3	Fine	7.8
8	Iron	600	7	0.8	1.9	4.3	Fine	7.8
9	Silica	300	3.5	62.2	72.8	84.8	Coarse	2.19
10	Silica	300	3.5	32.5	41.4	51.9	Fine	2.19
11	Silica	300	7	62.2	72.8	84.8	Coarse	2.19
12	Silica	300	7	32.5	41.4	51.9	Fine	2.19

3. Results and discussion

The image processing developed here allows for extracting a wide range of information useful in defining cloud dynamics. This paper will focus mainly on the motion field of the cloud in the area between the electrodes because it is a key parameter for assessing the behavior of a flame kernel in the initial stages of propagation (stretching, quenching…). More generally, a better understanding of cloud dynamics is essential when determining explosion parameters because, in addition to affecting the initial step of the flame propagation, as mentioned above, it modifies the local concentration of the cloud as well as the particle size distribution.

3.1. Cloud dynamics

Fig. 3 and Fig. 4 clearly illustrate how the standard MIE measurement procedure [4,7] may be further optimized, as dust cloud ignition "optimal" conditions may vary according to different parameters (e.g., dispersion pressure, ignition delay time). Since light intensity is directly correlated to the dust cloud concentration, it can be seen from Fig. 1 that dust concentration is not steady after 60 ms from the air blast. Maximum dust concentration peaks repeatedly from the early dispersion phase up to about 170 ms, finally stabilizing from 200 ms on when a "steady" state is reached.

Dust concentration and turbulence intensity are relevant parameters of ignition likelihood. If cloud lift only is considered (Fig. 4), it is worth noting that, at the ignition time, the cloud front has already risen above the electrodes. Still, no other information is displayed about the dust cloud distribution and turbulence at that time. Only average and maximum intensity values could be estimated and reported to indicate the variation of this parameter at ignition time.

3.2. Velocity of particles and flow dynamics

Instantaneous dust cluster velocity is estimated through the algorithm presented in section 1.3. Fig. 5 shows the vertical *v(t)* and horizontal velocity *u(t)* components in the area between the two electrodes. As expected, the horizontal component has significant turbulent oscillations around an average value of almost zero in any time interval. The vertical velocity component has much more marked oscillations than the horizontal component, around average values that are positive in the first phase and become negative in the second phase of dispersion. This trend is consistent with the dynamics of the cloud, which has a first ascending phase followed by a phase during which the particles move substantially in free fall.

The results obtained by ISM are generally consistent with those in the literature. For example, using Particle Image Velocimetry (PIV) on starch particles with a mean diameter of 25 μm, Cuervo [6] observed vertical velocities v(t) between -0.5 m.s^{-1} and 1.5 m.s^{-1}, and horizontal components u(t) varying between -0.5 m.s^{-1} and 0.5 m.s^{-1}. The same author determined that for coarse glass beads (d_{50} = 86 μm), horizontal components u(t) fluctuate around 0 ± 0.7 m.s^{-1}, while vertical velocities range from -0.5 to 3.5 m.s^{-1}. It should be noted that if u(t) values are in line with the results shown in Fig. 5, v(t) values reported for glass beads are higher than those obtained in test 11, i.e. a maximum of 1.5 m.s^{-1}. Schweitzer et al. [11] used Digital In-line Holography (DIH) combined with PIV to determine velocity fields of fine aluminum particles (d_{50} < 30 μm) in a MIKE3 tube. They recorded instantaneous velocities in the vertical direction ranging from 0 to 1 m.s^{-1}, and planar velocities (in the laser sheet observation plane) ranging from 0 to 2 m.s^{-1}. Finally, average velocities varying between 0 and 3 m.s^{-1} were determined by Hosseinzadeh et al. [12] using PIV on fine TiO_2 powders. Although based on different techniques and powders, these results from the literature confirm the orders of magnitude obtained by ISM.

The comparison between the tests presented in Fig. 5 allows some interesting considerations. Dotted lines were added to highlight the

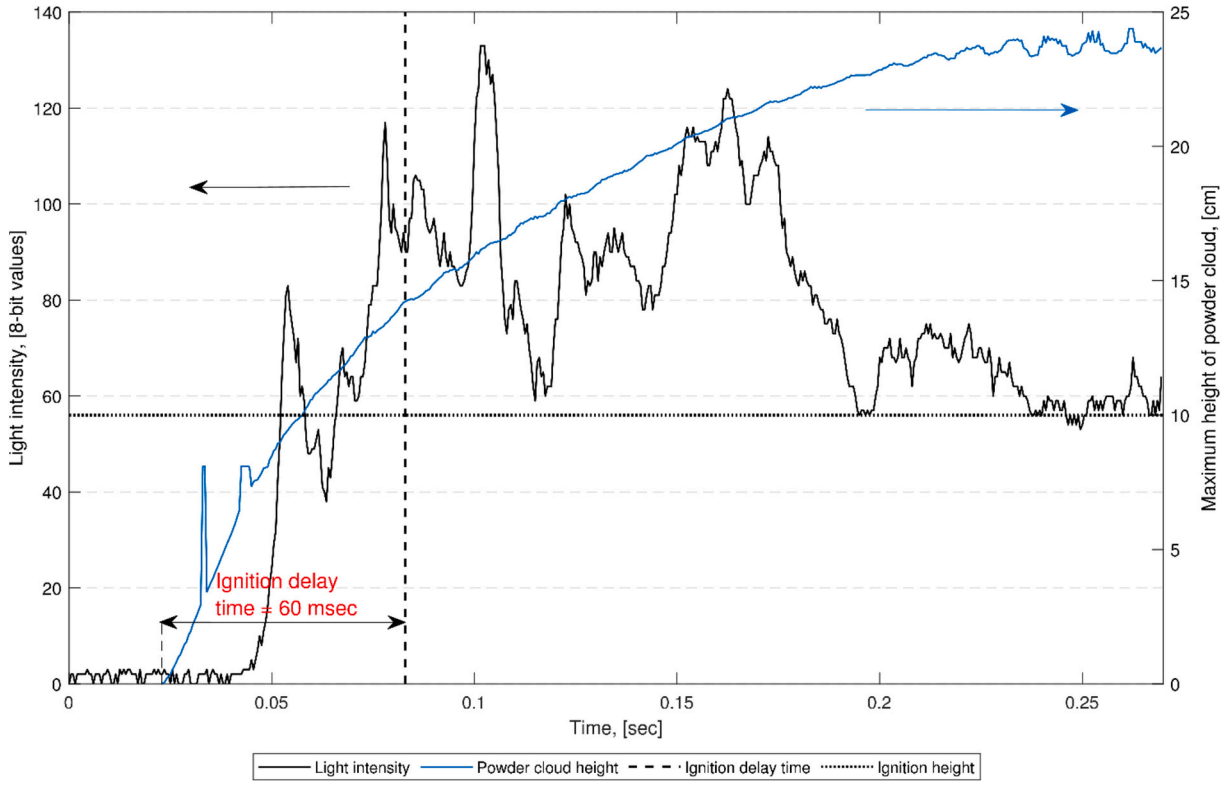

Fig. 3. Test #10 (silica): evolution of the light intensity of the dust cloud dispersion and maximum height of powder cloud, based on the algorithm developed by Danzi et al. [3].

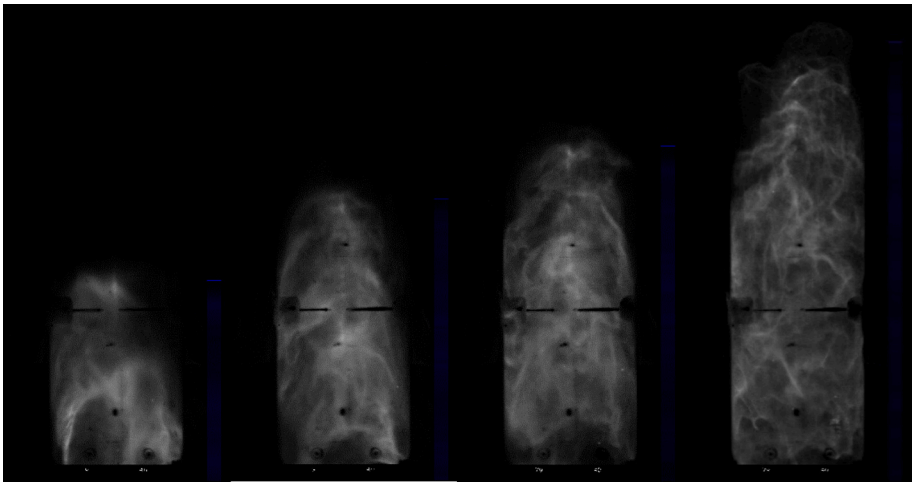

Fig. 4. Test #10 (silica) shows the evolution of the dust cloud in the tube at 60, 90, 150, and 210 ms after the sample's dispersion.

variation range of the ignition delay time, as defined by EN ISO/IEC 80079–20-2 standard [4], i.e., between 60 and 180 ms. Obviously, as the dispersion pressure increases, the velocity value and the root mean square u' increase. This effect testifies to the increased turbulence that occurs during high-pressure dispersions. However, high-pressure blasts cause dust dispersion to happen faster and speed fluctuations to decay faster (compare tests #1 and 2, 3 and #4, 9 and 11, 10 and 12). Further discussion will follow in the next paragraph. It is very interesting to compare tests carried out at the same pressure using powder of different sizes. In this case, the smaller the size of the dust, the wider the initial speed fluctuations (compare tests # 9 and 10, 11 and 12). In the case of fine dust, speed fluctuations decay faster than with coarse dust. Experiments with iron powders produced low-contrast films because of the powder's color. For this reason, the information obtained by processing the videos is more difficult to analyze.

Video analysis and determination of velocity components as a function of time provide a better understanding of particle distribution in the flow. Considering the Hartmann tube diameter as the characteristic flow dimension L_c, it is possible to calculate the Stokes number for the entire particle size distribution of a powder:

$$Stk = \frac{\rho_p . d_p^2 . u_g}{18 . \mu_g . L_c} \tag{2}$$

where ρ_p is the particle density, d_p, the diameter (which will be varied to cover the whole PSD), u_g and μ_g the gas velocity and dynamic viscosity, respectively. For Stokes numbers greater than unity, the particles will be detached from the gas streamlines and can be considered inertial particles, whereas, for Stokes lower than 0.1, the particles will follow the gas flow accurately (tracer accuracy error lower than 1 %). It should be noted that such analysis is valid for a single particle and does not consider the influence of dust concentration. However, the effect of the presence of other particles on the terminal velocity of powder was quantified using Richardson-Zaki relationship [13]; at the concentrations considered, deviations are less than 1 %. Moreover, physical interactions between particles of different sizes during dispersion/settling, although existing [14], will not be considered here.

In the case of coarse iron (#5 and 6, Fig. 6), it is clear that for gas velocities of 0.3 $m.s^{-1}$, the fraction with a size below 30.8 μm can be considered as flow tracers, while a Stokes number of 1 is not achievable on the PSD under consideration. For example, the air injection pressure would have to be increased until gas velocities of 1.5 $m.s^{-1}$ were obtained for particles larger than 44.2 μm to be equivalent to inertial particles. ISM analyses (tests #5 and 6, Fig. 5) show that these conditions are not achievable over the pressure range considered.

A similar analysis can be performed for each powder and, for instance, for coarse silica (Fig. 7). For the different tests carried out with this powder, the maximum vertical velocity ranges from 1.2 to 1.7 $m.s^{-1}$ after 60 ms to approximately 0.1–0.3 $m.s^{-1}$ at 180 ms (tests #9 and 11, Fig. 5). For ignition delay time t_v equal to 60 ms, only particles with a smaller diameter than 25 μm (a negligible part) will behave as pure flow-tracers. In contrast, particles with a diameter greater than 79.2 μm will be considered inertial particles, detaching from the streamline. At 180 ms, the same analysis leads to the following conclusion: coarse silica particles will never be detached clearly from the flow (which now mostly flows downwards), and particles with diameters lower than 59.5 μm will be considered perfect tracers of the gas flow. This analysis, albeit theoretical since silica is not combustible, shows that choosing an ignition delay time has clear consequences on the behavior of the particles in the particle-laden flow. Indeed, in addition to modifying the cloud's initial turbulence, the choice of t_v can increase or smooth out powder segregation phenomena as a function of their diameter within the tube. Due to the strong influence of particle diameter on MIE [15], such local PSD variations can lead to ignition sensitivity changes.

However, particle size is not the only criterion to consider: particle density also has a leading role, as Portarapillo et al. [16] highlighted when studying particle sedimentation in the 20-L explosion vessel. It should be noted that the density of starch is much lower than that of silica or iron (Table 1). For starch (Fig. 8), at gas velocities equal to those previously considered, the flow properties do not allow a Stokes number of 1 to be reached; this is also true at gas velocities as high as 3 $m.s^{-1}$. Moreover, particles smaller than 35 μm (limit set at 46.2 μm when u_g = 2 $m.s^{-1}$) can all be considered tracer-particles. This is in line with the findings of Portarapillo et al. [16]: the flow behavior of powders with a density of less than 1000 $kg.m^{-3}$ is unaffected by their size. However, our analysis shows that, contrary to the limit set at 100 μm by previous authors, the value below which the effects of density can be neglected can be as low as 30 to 40 μm as a function of the gas velocity. Nevertheless, it should be kept in mind that their analysis was done for the 20-L explosion vessel, for which dispersion conditions are more severe, even leading to the fragmentation of agglomerates and brittle particles [17].

The previous analysis of Stokes numbers shows the influence of particle size distribution on whether or not the powders studied can be considered as flow tracers. It therefore shows whether the characteristics observed are those of the fluid as well as those of the gas (in the case of a low Stokes number) or are attributable solely to the particles (if the powders are not flow tracers). As with the PIV technique, whose results are strongly dependent on the powder's representative Stokes number distribution, ISM is also dependent on the span of the distribution. The

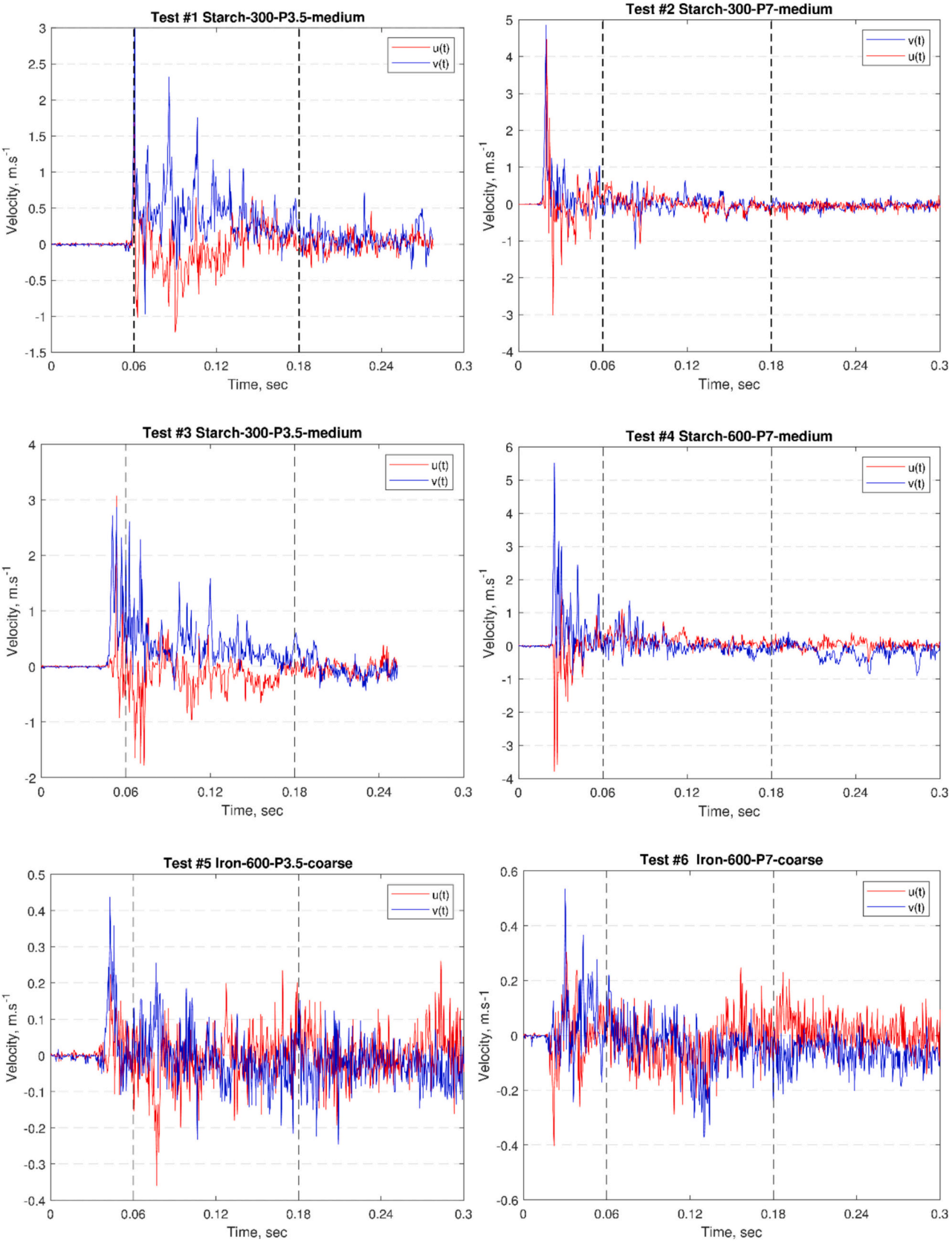

Fig. 5. Velocity components for different dispersion tests.

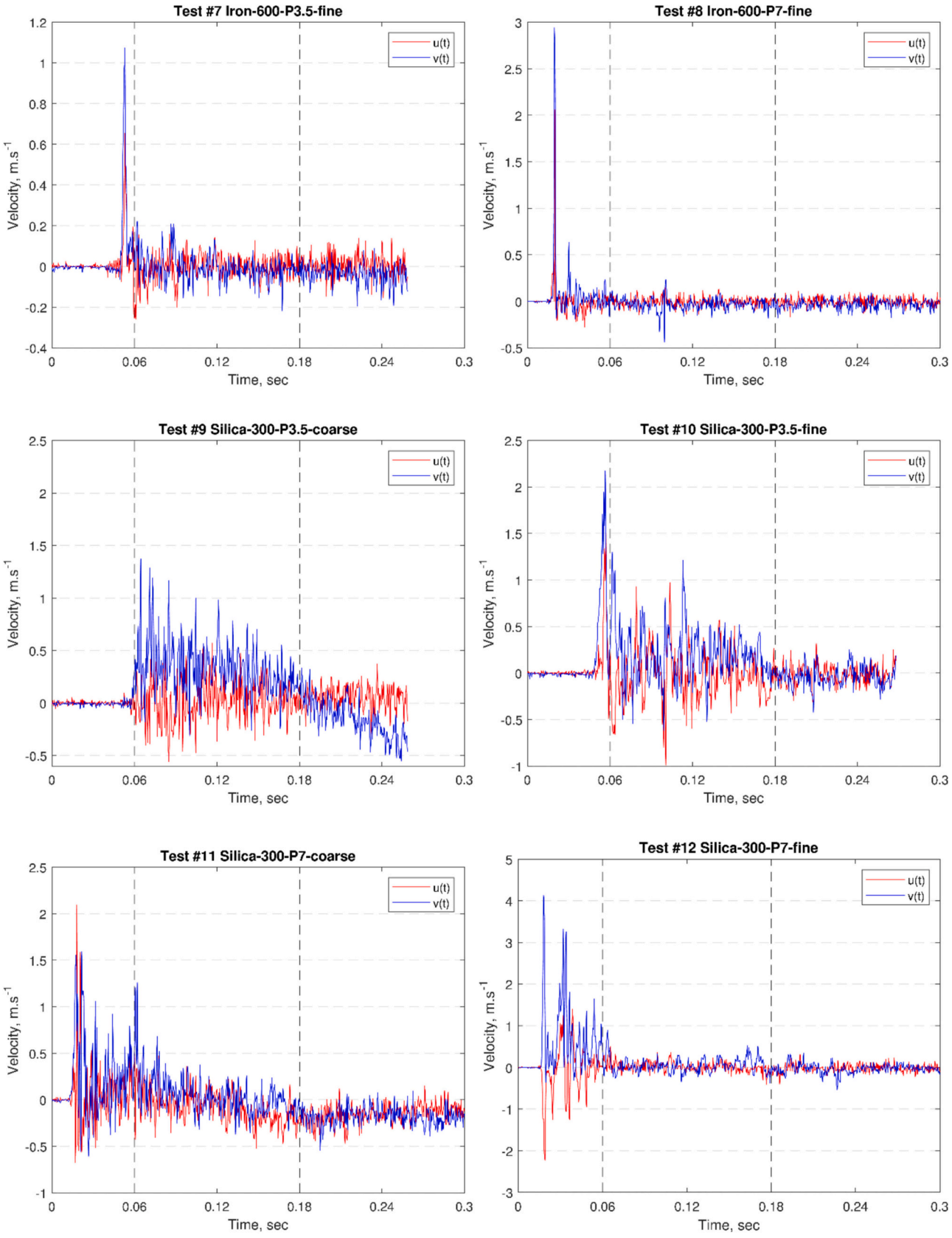

Fig. 5. (*continued*).

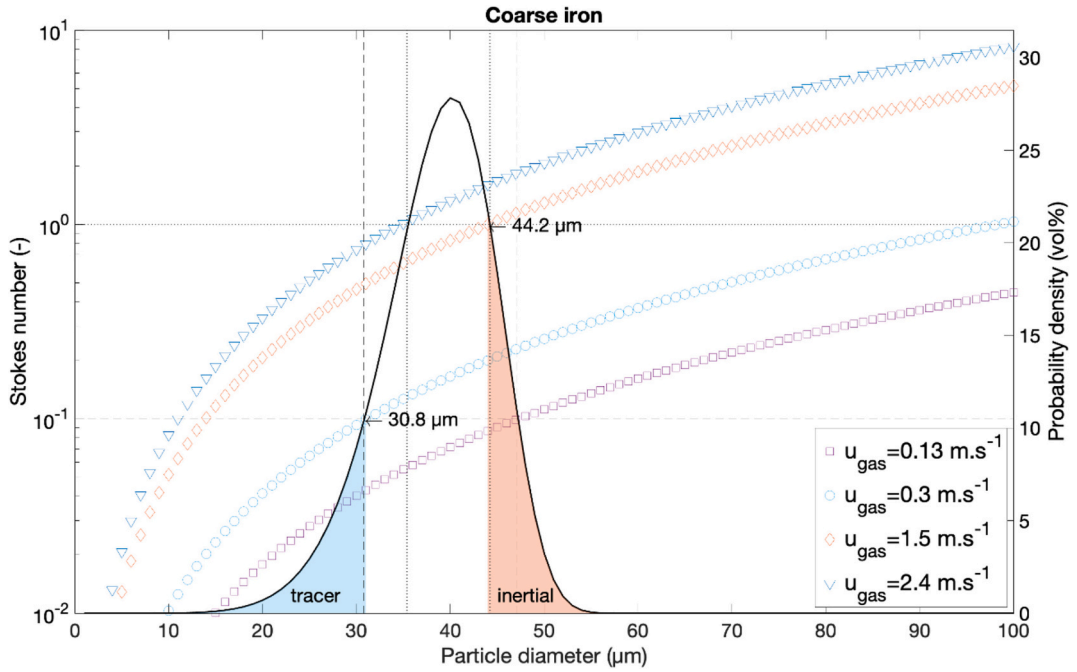

Fig. 6. Coarse iron: Stokes number evolution as a function of the particle diameter at different gas velocities.

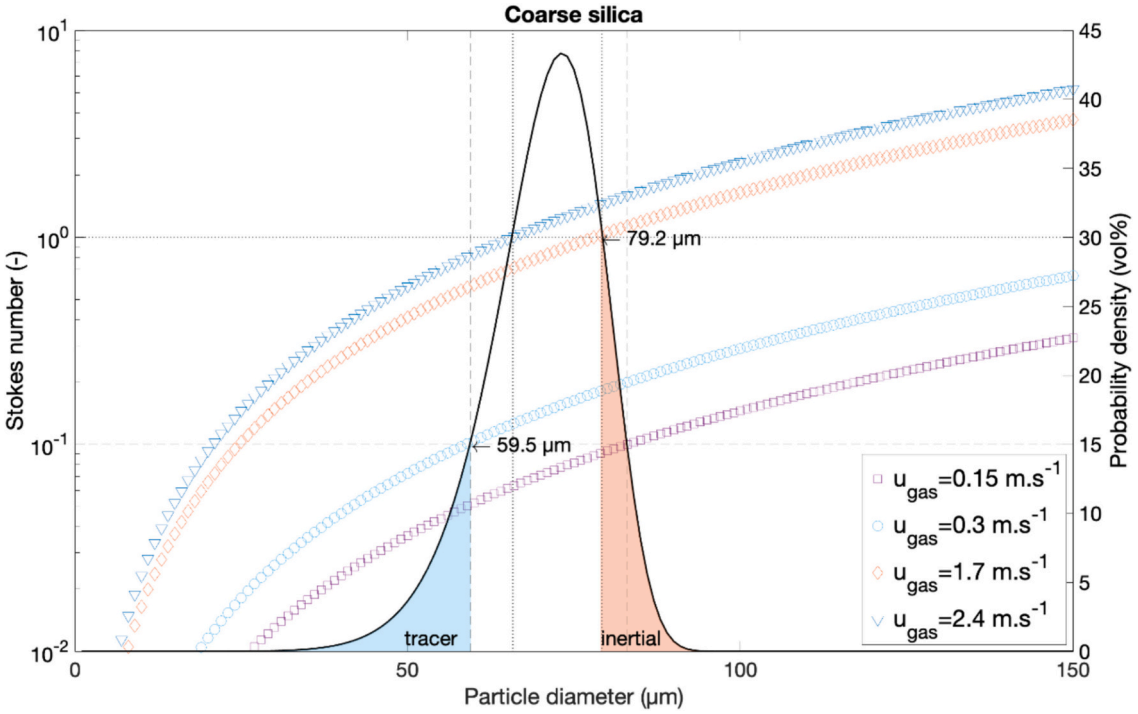

Fig. 7. Coarse silica: Stokes number evolution as a function of the particle diameter at different gas velocities.

use of fine powders, with a Stokes number of less than 0.1 or even 1, and with a small span, is therefore recommended when using ISM. However, it should also be kept in mind that, in the specific case of dust explosion, the velocity-components of the particles are also of interest, even if they cannot be considered as flow tracers.

3.3. Instantaneous kinetic energy

The speed fluctuations shown in Fig. 5 characterized the cloud's turbulence. As is known, the speed fluctuations are used in a stationary motion field to represent the turbulence intensity I according to the following equation:

$$I = u'/\overline{U} \tag{3}$$

where u' is the root mean square (or standard deviation) of the velocity fluctuations at a particular location during a specified time interval, while $\overline{U}$ is the average velocity in the same location calculated over the same time interval.

In the case of dust dispersion in the modified Hartmann tube, the

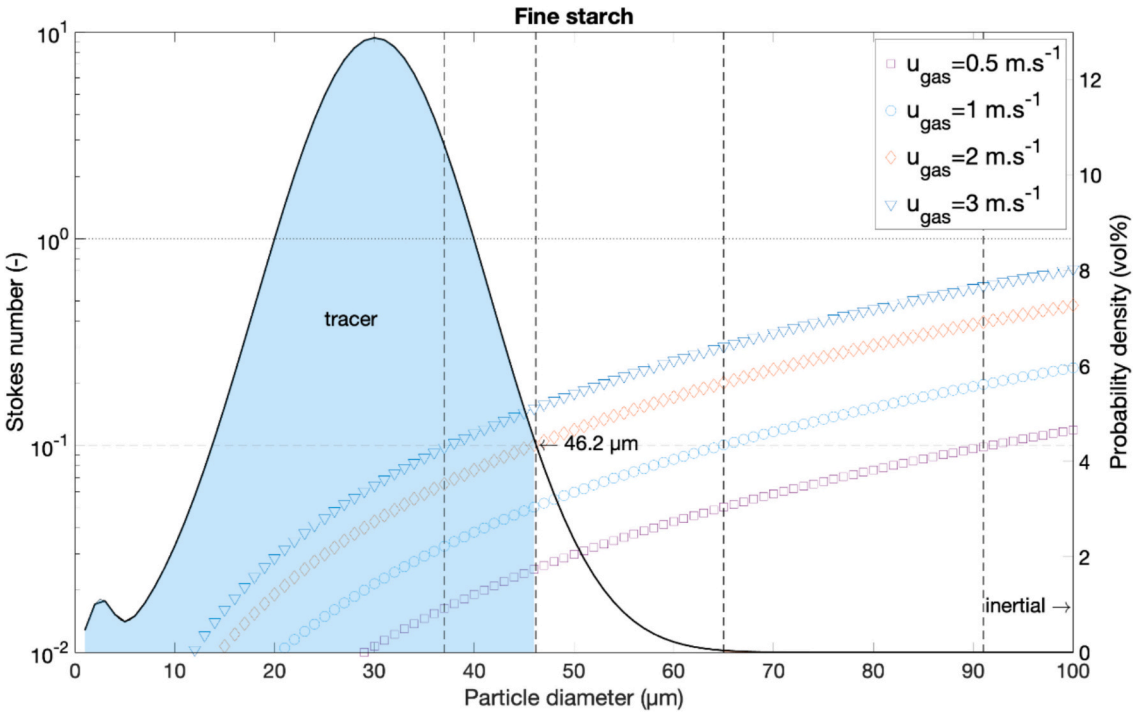

Fig. 8. Fine starch: Stokes number evolution as a function of the particle diameter at different gas velocities.

cloud motion is strongly non-stationary, which makes the estimate of $\overline{U}$ unreliable. Particularly in the horizontal plane, the mean velocity fluctuates around zero, as demonstrated by Cuervo [6] and Schweitzer et al. [11]. Indeed, the latter authors have shown that in the MIKE3 tube, the average x-component velocity was 0.05 ± 0.05 m.s^{-1}, whereas the average z-component velocity (still in the horizontal plane) was −0.07 ± 0.16 m.s^{-1}, which shows that these values are difficult to distinguish from zero. Therefore, the turbulence intensity cannot be estimated appropriately in our case, but u' can still be determined.

On the contrary, it is possible to estimate the instantaneous turbulent kinetic energy (*IKE*) in the observation plane using the equation shown below, where only the two components of the velocity vector appear that the experimentation allows to determine (horizontal and vertical).

$$IKE = \frac{1}{2} \bullet \left(\sigma_x^2 + \sigma_y^2\right) = \frac{1}{2} \bullet \left(\overline{u'^2} + \overline{v'^2}\right) \quad (4)$$

where σ is the standard deviation along the different spatial coordinates, and each turbulent velocity component (u', v') is the difference between the instantaneous (u) and the average velocity ($\overline{u}$):

$$u' = u - \overline{u} \quad (5)$$

Fig. 9 shows the time course of *IKE* in the various tests. The *IKE* is calculated at a point on the diameter of the modified Hartmann tube, at the height of the electrodes, so that it represents turbulence at the point where the electric arc is generated.

The *IKE* trend is very interesting: as expected, there is a clear maximum when the cloud reaches the point of interest. Then, the *IKE* decreases to almost negligible values. It is especially worth comparing *IKE* values calculated in different test conditions.

3.3.1. The effect of the blast pressure

By comparing tests at different pressures, it is evident that the dispersion pressure generates turbulence (compare tests #1 and 2, #3 and 4, #9 and 11, #10 and 12, Fig. 9). Therefore, high-pressure tests have higher *IKE* at the early phase of dispersion. *IKE* maximum more than doubles, passing from 3.5 bar to 7 bar dispersion pressure. Regarding the same tests, the *IKE* decays faster when the jet is carried out at high pressure. These results are consistent with the maximum values of turbulent kinetic energy determined by Murillo [18] on wheat starch, although the decay observed here is faster. Indeed, IKE of up to 30 m^2.s^{-2} have been reported by Murillo [18], with specific IKE values varying from 20 m^2.s^{-2} to 10 m^2.s^{-2} at electrode height for a decay period of 35 ms. At typical MIE determination time (e.g., 90–180 ms delay time), *IKE* has significantly decayed in all runs at 3.5 and 7 bar. As *IKE* decays quickly at higher pressure blasts, after 60 ms, runs performed at 7 bar apparently exhibit a lower *IKE* than runs at 3.5 bar.

3.3.2. The effect of dust properties

Dust PSD significantly affects the *IKE*. Comparing tests conducted with "*fine*" and "*coarse*" dust (#9 and 10, 11 and 12), it is clear that tests carried out with *"fine"* dust show *IKE* much greater than tests carried out with "coarse" dust. Also, the decay of *IKE* is slower in the case of "*fine"* dust. As a result, after 60 ms (but also after 180 ms) from the jet, the *IKE* value is much higher in the case of "*fine"* dust. This may be because smaller particles have less inertia and, therefore, shorter characteristic time and low Stokes number, as described in section 2.2. Thus, smaller particles can better follow turbulent gas fluctuations than larger ones, meaning they perceive the lower-scale turbulence of the gas phase and follow fluid streamlines. The same phenomenon is observed in tests carried out at low or high pressure (3.5 or 7 bar) jet pressure. The effect of density is also noticeable: as particle density increases, *IKE* tends to decrease due to a larger Stokes number (Eq. 2).

3.4. Optimal conditions for MIE measurement

As previously noted, the optimal conditions for measuring the MIE include homogeneous concentration and turbulence as low as possible to improve the stability of the flame kernel and its propagation. Due to the transient nature of the cloud in the modified Hartmann tube, these conditions are only met over a limited period.

During the initial phase, the cloud is very heterogeneous, with high turbulence. In the final stages, the cloud has very low turbulence because, basically, the particles fall in free fall. The concentration at the

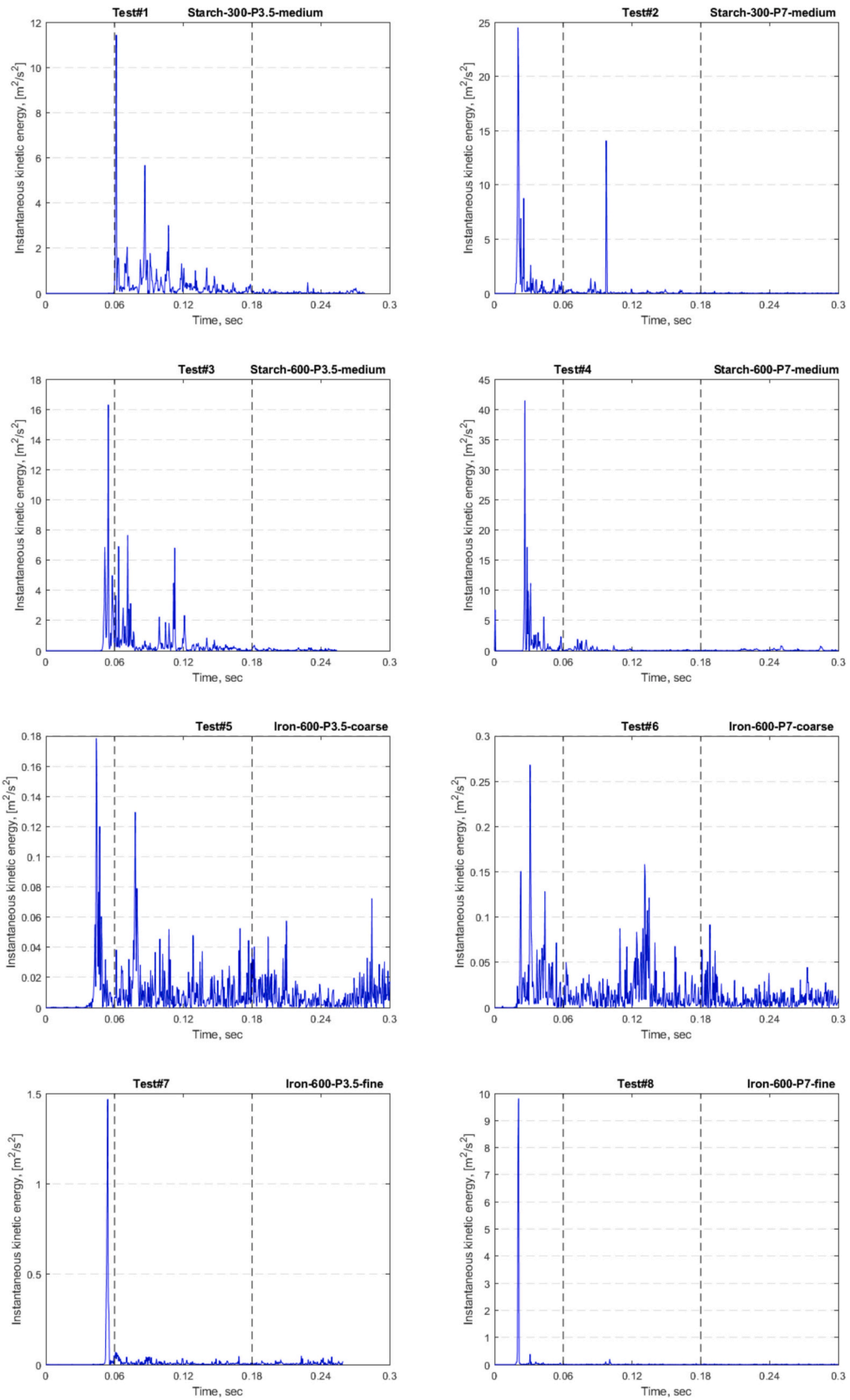

Fig. 9. Turbulent kinetic energy (IKE) calculated at different dispersion conditions.

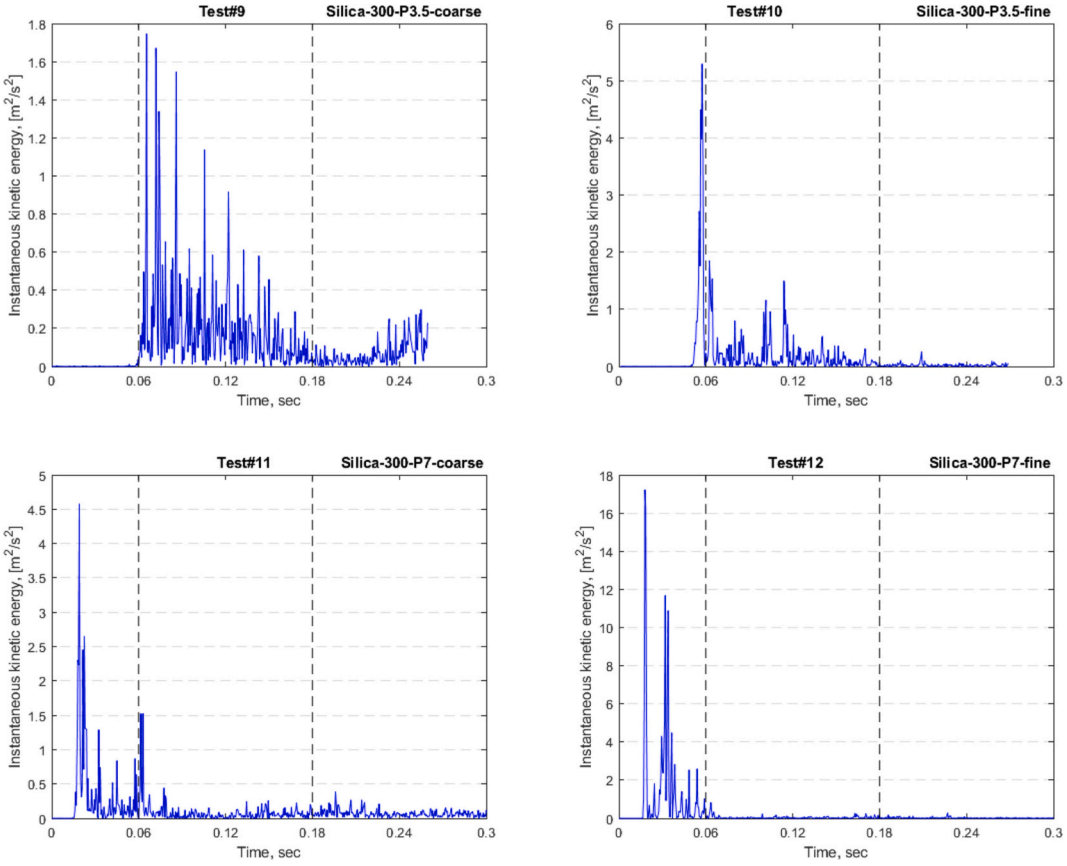

Fig. 9. (*continued*).

electrode level decreases, and the cloud becomes heterogeneous again. There is an intermediate phase during which turbulence (*IKE*) is significantly reduced, and the cloud is practically homogeneous. This is the optimal phase for measuring the MIE. However, numerous operational variables influence the duration of this phase. Some are already defined by current standards (blast pressure); others, such as PSD, are not controllable a priori. Since the decay rate of the *IKE* depends on the particle's properties, the optimal delay time for measuring MIE should likely be adjusted according to their PSD, particle shape, and density. It should be noted, however, that for samples consisting either of pure powder with a wide particle size distribution or of multiple compounds of varying density and PSD, it is unlikely to combine homogeneity and low turbulence in this type of device. Finally, another parameter, the irregular or smooth surface of powders, has a marked impact on turbulence and concentration distribution in the cloud [19]. This aspect, which has not been considered here, can also be addressed using ISM.

4. Conclusion

This work presented a post-treatment method for high-speed films of Hartmann tube dust clouds. The developed algorithm extracts information about the local components of the instantaneous dust velocity, from which turbulent speed fluctuations and turbulent kinetic energy (*IKE*) can be traced. This method offers an accessible alternative to optical methods such as particle image velocimetry (PIV) without achieving the same definition but with a lower cost.

A comparison of tests carried out at different blast pressures, concentrations, and types of solid showed the effects of the main variables on cloud dynamics. The blast pressure increases the initial turbulence, but it decays faster than at low blast pressures. Fine dust leads to more turbulence, which decays more slowly.

These preliminary indications require cross-confirmation by comparison with other methods of measuring cloud turbulence. In any case, these results provide useful indications to optimize the measurement procedure of the MIE. This work confirms that it is imperative to vary ignition delay times over wide turbulence ranges during MIE tests to increase the chances of testing the dust under "optimal" conditions. A good indicator for defining such conditions for determining the MIE may be the Stokes number, or more likely the Stokes numbers associated with the particle size distribution of the sample.

CRediT authorship contribution statement

Luca Marmo: Writing – review & editing, Writing – original draft, Validation, Supervision, Methodology, Investigation, Formal analysis, Data curation, Conceptualization. **Olivier Dufaud:** Writing – review & editing, Writing – original draft, Validation, Investigation, Formal analysis, Data curation, Conceptualization. **Fausto Franchini:** Writing – original draft, Visualization, Software, Data curation. **Enrico Danzi:** Writing – original draft, Validation, Investigation, Formal analysis, Data curation.

Declaration of competing interest

The authors declare the following financial interests/personal relationships which may be considered as potential competing interests:

Luca Marmo reports financial support was provided by Polytechnic of Turin Department of Applied Science and Technology. Enrico Danzi reports financial support was provided by Polytechnic of Turin Department of Applied Science and Technology. Fausto Franchini reports financial support was provided by Polytechnic of Turin Department of Energy. Olivier Dufaud reports financial support was provided by Université de Lorraine. If there are other authors, they declare that they have no known competing financial interests or personal relationships

that could have appeared to influence the work reported in this paper.

Data availability

Data will be made available on request.

References

[1] P.R. Amyotte, M.J. Pegg, Lycopodium dust explosions in a Hartmann bomb: effects of turbulence, J. Loss Prev. Process Ind. 2 (2) (1989) 87–94, https://doi.org/10.1016/0950-4230(89)80004-X.

[2] E. Danzi, F. Franchini, O. Dufaud, M. Pietraccini, L. Marmo, Investigation of the fluid dynamic of the modified Hartmann tube equipment by high-speed video processing, Chem. Eng. Trans. 86 (2021) 367–372, https://doi.org/10.3303/CET2186062.

[3] E. Danzi, F. Franchini, O. Dufaud, M. Pietraccini, L. Marmo, Study of dust cloud behaviour in the modified Hartmann tube using the image subtraction method (ISM), J. Loss Prev. Process Ind. 82 (2023) 104997, https://doi.org/10.1016/j.jlp.2023.104997.

[4] EN ISO/IEC 80079-20-2:2016, Explosive Atmospheres - Part 20–2: Material Characteristics - Combustible Dusts Test Methods, International Organization for Standardization, 2016.

[5] P.R. Amyotte, S. Chippett, M.J. Pegg, Effects of turbulence on dust explosions, Prog. Energy Combust. Sci. 14 (4) (1988) 293–310, https://doi.org/10.1016/0360-1285(88)90016-0.

[6] N. Cuervo, Influences of Turbulence and Combustion Regimes on Explosions of Gas- Dust Hybrid Mixture, PhD Thesis (in English), University of Lorraine, Nancy, France, 2015.

[7] ASTM E2019-03, Standard test method for minimum ignition energy of a dust cloud in air, Am. Soc. Test. Mater. (2019), https://doi.org/10.1520/E2019-03R19.

[8] Y. Pan, C. Spijker, H. Raupenstrauch, CFD modeling of particle dispersion behavior in the MIKE 3 apparatus, Alex. Eng. J. 61 (12) (2022) 9305–9313, https://doi.org/10.1016/j.aej.2022.03.039.

[9] S. Puttinger, C. Spijker, S. Schneiderbauer, S. Pirker, G. Meyer, C. Buchner, A. Kerbl, Dust cloud evolution and flame propagation of organic dust deflagration under low wall influence, J. Loss Prev. Process Ind. 83 (105042) (2023) 950–4230, https://doi.org/10.1016/j.jlp.2023.105042.

[10] B.K.P. Horn, B.G. Schunck, Determining optical flow, Artif. Intell. 17 (1–3) (1981) 185–203, https://doi.org/10.1016/0004-3702(81)90024-2.

[11] C. Schweizer, C.V. Mashuga, W.D. Kulatilaka, Investigation of aluminum dust cloud dispersion characteristics in an explosion hazard testing device using laser-based particle and flow diagnostics, Process. Saf. Environ. Prot. 166 (2022) 310–319, https://doi.org/10.1016/j.psep.2022.08.013.

[12] S. Hosseinzadeh, M. Vanierschot, F. Norman, F. Verplaetsen, J. Berghmans, Flame propagation and flow field measurements in a Hartmann dust explosion tube, Powder Technol. 323 (2018) 346–356, https://doi.org/10.1016/j.powtec.2017.10.001.

[13] M.J. Lockett, K.S. Bassoon, Sedimentation of binary particle mixtures, Powder Technol. 24 (1) (1979) 1–7, https://doi.org/10.1016/0032-5910(79)80001-7.

[14] T.N. Smith, Differential settling of a binary mixture, Powder Technol. 92 (2) (1997) 171–178, https://doi.org/10.1016/S0032-5910(97)03236-1.

[15] W. Kim, R. Saeki, Y. Ueno, T. Johzaki, T. Endo, K. Choi, Effect of particle size on the minimum ignition energy of aluminum powders, Powder Technol. 415 (2023) 118190, https://doi.org/10.1016/j.powtec.2022.118190.

[16] M. Portarapillo, R. Sanchirico, A. Di Benedetto, Dust particle sedimentation in the 20 L standard vessel for dust explosion tests, J. Loss Prev. Process Ind. 83 (2023) 105016, https://doi.org/10.1016/j.jlp.2023.105016.

[17] Q. Yuan, Y. Bu, P. Amyotte, Z. Dong, C. Li, H. Chen, Z. Liu, G. Li, W. Hu, C. Yuan, Effect on ignition sensitivity of combustible dust particle size reduction due to dispersion in the 20-L chamber, Powder Technol. 433 (2024) 119188, https://doi.org/10.1016/j.powtec.2023.119188.

[18] C. Murillo, Experimental and Numerical Approaches to Particles Dispersion in a Turbulent Flow: Application to Dust Explosions, PhD Thesis (in English), University of Lorraine, Nancy, France, 2016.

[19] S. Prasad, C. Schweizer, P. Bagaria, W.D. Kulatilaka, C.V. Mashuga, Effect of particle morphology on dust cloud dynamics, Powder Technol. 379 (2021) 89–95, https://doi.org/10.1016/j.powtec.2020.10.058.